The gut microbiota ellagic acid-derived metabolite urolithin A, and its sulfate conjugate, are substrates for the drug efflux transporter breast cancer resistance protein (ABCG2/BCRP).

Journal:	*Journal of Agricultural and Food Chemistry*
Manuscript ID:	jf-2013-007505
Manuscript Type:	Article
Date Submitted by the Author:	15-Feb-2013
Complete List of Authors:	González-Sarrías, Antonio; CEBAS-CSIC, Food Sci. & Technol. Miguel, Veronica; University of Leon, Department of Biomedical Sciences (Physiology) Merino, Gracia; University of Leon, Department of Biomedical Sciences-Physiology Lucas, Ricardo; Instituto de Investigaciones Químicas, CSIC - Universidad de Sevilla, Química Bioorgánica Morales, Juan; Instituto de Investigaciones Químicas, CSIC - Universidad de Sevilla, Química Bioorgánica Tomás-Barberán, Francisco; CEBAS-CSIC, Alvarez, Ana I.; University of Leon, Department of Biomedical Sciences (Physiology) Espín, Juan C.; CEBAS-CSIC, Food Sci. & Technol.

The gut microbiota ellagic acid-derived metabolite urolithin A, and its sulfate conjugate, are substrates for the drug efflux transporter breast cancer resistance protein (ABCG2/BCRP).

ANTONIO GONZÁLEZ-SARRÍAS[†], VERÓNICA MIGUEL[‡], GRACIA MERINO[‡], RICARDO LUCAS[#], JUAN C. MORALES[#], FRANCISCO TOMÁS-BARBERÁN[†], ANA I. ÁLVAREZ[‡], JUAN C. ESPÍN[†]*

[†]Research Group on Quality, Safety and Bioactivity of Plant Foods, Dept. Food Science and Technology, CEBAS-CSIC, P.O. Box 164, 30100 Campus de Espinardo, Murcia, Spain; [‡]Department of Biomedical Sciences-Physiology, Campus Vegazana, University of León, 24071 León, Spain and [#]Department of Bioorganic Chemistry, Institute of Chemical Research, CSIC-University of Seville, 41092 Seville, Spain.

***Corresponding author**: Juan Carlos Espín, Research Group on Quality, Safety and Bioactivity of Plant Foods, Dept. Food Science and Technology, CEBAS-CSIC, P.O. Box 164, 30100 Campus de Espinardo, Murcia, Spain. Tel: +34 968 396344. Fax. +34-968 396213. E-mail address: jcespin@cebas.csic.es

RUNNING TITLE: Urolithins and ABCG2/BCRP transporter

ABSTRACT

The breast cancer resistance protein (BCRP/ABCG2) is a drug efflux transporter that can affect the pharmacological and toxicological properties of many molecules. Urolithins, metabolites produced by the gut microbiota from ellagic acid (EA) and ellagitannins, have been acknowledged with *in vivo* anti-inflammatory and cancer chemopreventive properties. We here evaluated whether urolithins (Uro-A, -B, -C and -D), their main phase II metabolites Uro-A sulfate, Uro-A glucuronide, and Uro-B glucuronide as well as their precursor EA were substrates for ABCG2/BCRP. Parental and Bcrp1-transduced MDCKII cells were used for active transport assays. Uro-A, and in a lesser extent Uro-A sulfate, showed a significant increase in apically directed translocation in Bcrp1-transduced cells. Bcrp1 did not show affinity for the rest of tested compounds. Data were confirmed for murine, human, bovine and ovine BCRP-transduced subclones as well as with the use of the selective BCRP inhibitor Ko143. The transport inhibition by Uro-A was analyzed by flow cytometry compared to Ko143 using the antineoplastic agent mitoxantrone as a model substrate. Results showed that Uro-A was able to inhibit mitoxantrone transport in a dose-dependent manner. We report here for the first time that Uro-A and its sulfate conjugate are ABCG2/BCRP substrates. Our results suggest that physiologically relevant concentrations of these gut microbiota-derived metabolites could modulate ABCG2/BCRP-mediated transport processes and mechanisms of cancer drug resistance. Further *in vivo* investigations are warranted.

KEYWORDS: *Urolithin; ellagic acid; ABCG2/BCRP transporters; gut microbiota; Bcrp1-MDCKII cells.*

INTRODUCTION

ABCG2/BCRP is an ATP-binding cassette (ABC) transporter that mediates energy-dependent translocation of substrates from cells in the intestine, liver, kidney, mammary gland, etc. across cellular membranes, affecting the pharmacokinetics and disposition of drugs and other compounds such as xenotoxins, endogenous compounds, etc. in tissues, and mediating drug-drug interactions.[1,2] The multifunctional behavior of ABCG2/BCRP linked to great substrate specificities for a wide range of compounds supported its important role in homeostatic processes.[3,4] In addition, the modulation of ABCG2/BCRP transporters can affect chemotherapeutic treatments by modulating the pharmacokinetic behavior of anticancer drugs.[5-7]

Some *in vitro* and *in vivo* studies using BCRP-overexpressing cell lines and/or knockout mice have indicated that plant-derived polyphenols such as flavonoids and the stilbene resveratrol can interact directly with BCRP by modulating both its transport function and ATPase activity.[8-11] Recently, the important role of ABCG2/BCRP in the transport of glucuronide and sulfate conjugates of polyphenols including the flavonoids naringenin, genistein and daidzein,[12-14] as well as resveratrol conjugates[15] has been described.

Urolithins are dibenzopyran-6-one derivatives produced from ellagitannins and ellagic acid (EA) by the gut microbiota through the loss of one lactone ring present in EA and successive removals of hydroxyl groups[16-18] (**Figure 1**). Urolithins have been found in plasma, urine, feces and tissues in a number of animals including the pig,[19] rat,[20-22] mouse,[23] beef cattle,[24] etc. Urolithins are also produced by humans, and their occurrence has been reported in plasma, feces, urine,[16,18,25,26] and also prostate tissue[27] after the intake of ellagitannin-containing foods such as pomegranates, strawberries, raspberries, walnuts, and oak-aged wines. Phase II derived

conjugates of urolithins reach the plasma and systemic organs at low micromolar concentrations, whereas high concentrations of the aglycone forms can be found in the gut.[19,22]

In the last decade, after our first report about the occurrence of urolithins in humans,[16] numerous *in vitro* and *in vivo* studies have shown a wide range of biological activities of urolithins, mainly attributed to Uro-A, such as anticancer,[22,23,28-30] anti-inflammatory ,[31-35] anti-bacterial,[36] and estrogenic/anti-estrogenic.[37] However, the possible role of ABC transporters in the bioavailability of urolithins remains unknown.

Our aim was to evaluate whether ellagic acid (EA), urolithins A, B C and D (Uro-A, Uro-B, Uro-C and Uro-D) and their main glucuronide and sulfate derivates (Uro-A glucuronide, Uro-B glucuronide, and Uro-A sulfate) might be ABCG2/BCRP substrates, and/or inhibitors.

MATERIALS AND METHODS

Materials. Ellagic acid (EA) was purchased from Sigma-Aldrich (St. Louis, USA). Urolithin A (3,8-dihydroxy-6H-dibenzo[*b,d*]pyran-6-one; Uro-A) and urolithin B (3-hydroxy-6H-dibenzo[*b,d*]pyran-6-one; Uro-B) were synthesized as described previously.[38] Uro B glucuronide (Uro-B glur) was prepared according to Lucas et al. (2009).[39] Urolithin A glucuronide (Uro-A glur) and Urolithin A sulfate (Uro-A sulphate) were prepared as a mixture of regioisomers (**Figure 2**). Experimental procedure and ^{1}H-NMR data for the synthesis of Uro-A and Uro-A sulfate are detailed in **Supplementary Methods**. Briefly, Uro-A was first mono-protected with a silyl protecting group (**Figure 2A**). Random TBDMS-protection (*tert*-butyldimethylsilyl)[40] of Uro-A and subsequent chromatographic separation afforded the two possible mono-phenolic derivatives **1** and **2** as a regioisomeric mixture (1:1) and the double silylated Uro-A. The glycosylation reaction of acceptors **1** and **2** with glucuronosyl donor **3** was

performed using the same conditions described previously[39] to give compounds **4** and **5** as a regioisomeric mixture (83%). Ester hydrolysis and deprotection of acetyl and TBDMS groups were carried out in one step by using K_2CO_3 and KF in a methanol-water solution. Reverse phase purification of the crude afforded a 1:1 regioisomeric mixture of Uro-A 3-glucuronide and Uro-A 8-glucuronide (**Figure 2A**). Uro-A sulfate was also prepared as a mixture of regioisomers following a similar strategy to the one used for the glucuronate derivatives (**Figure 2B**). Sulfation of the mono-silylated urolithin derivatives **1** and **2** was carried out with SO_3•NMe_3 as sulfating reagent, NEt_3 as base, and acetonitrile as solvent at 100 ºC under microwave radiation for 20 min. The reaction afforded the sulfated 1:1 mixture of urolithin derivatives **6** and **7** in 92 % yield (**Figure 2B**). Final silyl deprotection with KF and reverse phase purification gave a 1:1 mixture of Uro-A 3-sulfate and Uro-A 8-sulfate (73% yield). Urolithin C (3,7,8-trihydroxy-6H-dibenzo[*b,d*]pyran-6-one, Uro-C) and urolithin D (2,3,7,8-tetrahydroxy-6H-dibenzo[*b,d*]pyran-6-one, Uro-D) were purchased from Dalton Pharma Services (Toronto, Canada). Purity was higher than 95% in all tested compounds. Dimethyl sulfoxide (DMSO), diethyl-ether and HPLC reagents, formic acid and acetonitrile (ACN), were obtained from Panreac (Barcelona, Spain). Methanol (MeOH) was from Lab-Scan (Gliwice, Poland). Ko143 was purchased from Tocris (Bristol, United Kingdom). Ultrapure Millipore water was used for all the experiments.

Cell Lines and Cell Culture Conditions. MDCKII cells (Mardin-Darby canine kidney) and their human BCRP-transduced and murine Bcrp1-transduced sub-clones were kindly provided by Dr. A.H. Schinkel, Netherlands Cancer Institute (Amsterdam). MDCKII cells stably transduced with bovine and ovine variants of ABCG2 have recently been generated by the research group.[41,42] Culture conditions were as previously described.[43] The cells were cultured in

93 Dulbecco's modified Eagle's medium (DMEM) containing GlutaMAX (Life Technologies, Inc.,
94 Madrid, Spain) and supplemented with penicillin (50 U/mL), streptomycin (50 μg/mL) and 10%
95 (v/v) fetal calf serum (MP Biomedicals; Cambridge, UK) at 37 °C in the presence of 5% CO2.
96 The cells were trypsinized every 3–4 days for sub-culturing. All of the test samples were
97 solubilized in DMSO (<0.5 % in the culture medium) and were filter sterilised (0.2 μm) prior to
98 addition to the culture media. Control cells were also run in parallel and subjected to the same
99 changes in medium with a 0.5 % DMSO.
100
101 **Transport studies.** Transepithelial transport assays using Transwell plates were carried out
102 as described previously[9,41] with minor modifications. Cells were seeded on microporous
103 polycarbonate membrane filters (3.0 μm pore size, 24 mm diameter; Transwell 3414; Costar) at a
104 density of 1.0×10^6 cells per well. Cells were grown for 3 days, and the medium was replaced
105 every day. Transepithelial resistance was measured in each well using a Millicell ERS ohmmeter
106 (Millipore). Wells registering a resistance of 200 Ω or greater, after correcting for the resistance
107 obtained in blank control wells, were used in the transport experiments. The measurement was
108 repeated at the end of the experiment to check the tightness of the monolayer.
109 Before the start of the experiment, medium on both sides of the monolayer was replaced with
110 2 mL of Optimem medium (Life Technologies), without serum. After 2 h pre-incubation, the
111 experiment was started by replacing the medium in either the apical or basolateral compartment
112 with fresh Optimem medium containing 20 μM of the compound tested (except the preliminary
113 screening which was performed at 10 μM). Aliquots of 100 μL were taken from the opposite
114 compartment at 2 and 4 h, and stored at −20 °C until LC-MS analysis. In the co-treatments

assays, the inhibitor Ko143 (1 μM) was added 2 h before each compound and remained during all experiment. Experiments were carried out in triplicate.

Accumulation assays. *In vitro* accumulation assays were carried out as described previouslyusing mitoxantrone (MXR, 10 μM) as fluorescent substrate.[44] In brief, subconfluent cultures were used after 36 h from seeding. Cells were incubated in Optimem medium with or without Ko143 inhibitor (1 μM) or EA, and urolithins A, B, C and D at different concentrations for 60 min before the addition of MXR. Accumulation of MXR was allowed for 1 h at 37°C. Then, cells were washed, trypsinized, collected and resuspended in PBS with 2.5% fetal calf serum. Relative cellular accumulation of MXR of at least 5,000 cells was determined by flow cytometry using a FACSCalibur cytometer (BD Biosciences, NJ, USA). Samples were gated on forward scatter vs. side scatter to exclude cell debris and clumps. Excitation and emission wavelengths for MXR were 635 and 650 nm, respectively. The fluorescence of the accumulated substrate in tested populations was quantified from histogram plots using the median of fluorescence (MF). At least three independent experiments were performed.

BCRP inhibition increases accumulation of MXR in Bcrp1/BCRP-transduced cells and thus increases MF. Possible background fluorescence of urolithins was checked in appropriate channels, but the fluorescence was negligible. Flow cytometry data were processed and analyzed using WinMDI version 2.8 software.

Percentage of inhibition was calculated according to the following equation: % inhibition = (MF with tested compound in BCRP cells-MF without tested compound in BCRP cells)/(MF with inhibitor Ko 143 in BCRP cells -MF without tested compound in BCRP cells) x 100.

Sample processing for the analysis of urolithins and their derivates. Cell media after transport studies was processed as described elsewhere.[34] Briefly, ACN (100 μL) was added to 100 μL of culture media, vortexed and centrifuged at 16,435×g for 10 min. The supernatant was then concentrated in a Speedvac® concentrator Savant SPD121P (Thermo Scientific, Alcobendas, Spain) and the residue re-dissolved in 100 μL of MeOH and filtered (0.45 μm) before analysis by LC-MS using the conditions described below.

LC-MS analysis. Aliquots of processed cell media were analyzed using a LC-MS system (1200 Series, Agilent Technologies, Madrid, Spain). The HPLC system was equipped with a 100 × 3 mm i.d., 2.7 μm, reverse phase C18 column (Poroshell 120, Agilent) and a single quadrupole mass detector in series (6120 Quadrupole, Agilent). Water:formic acid (99:1, v/v) and ACN were used as mobile phases A and B, respectively, with a flow rate of 0.5 mL/min. The linear gradient started with 5% of solvent B in solvent A, reaching 18% solvent B at 7 min, 28% at 17 min, 50% from 22 min, and 90% at 27 min which was maintained up to 29 min. The initial conditions were re-established at 29 min and kept under isocratic conditions up to 33 min. Injections (5 μL) were made for each sample at 25 ºC. The mass detector was a quadrupole mass spectrometer equipped with an ESI system (capillary voltage, 3.5Kv; dry temperature, 350 ºC; drying gas flow, 9 L/min; nebulizer pressure, 40 psi). MS spectra were measured in selective ion monitoring (SIM) mode using [M-H] ions for measuring all tested compounds. MS data were acquired in the negative ionization mode. Identification of all tested compounds was carried out by direct comparison (UV spectra and MS) with available standards and confirmed by their spectral properties, molecular mass and fragmentation pattern. Calibration curves were obtained for each tested

compounds with good linearity ($r^2 > 0.999$). EA was quantified at 360 nm, and urolithins and their conjugates at 305 nm using the corresponding available standards.

Statistical Analysis. All data are presented as mean values ± SD (n=3). Two-tailed unpaired Student's *t*-test was used for statistical analysis of the data. A p value < 0.05 was considered significant.

RESULTS

Initial screening of the transport of urolithins and EA on parental and Bcrp1-transduced MDCKII cell models. As initial screening, we used the polarized canine kidney cell line MDCKII and its subclone transduced with murine Bcrp1 cDNAs to test the possible role of Bcrp1 in the *in vitro* transport of EA, urolithins and some representative *in vivo* conjugates (**Figure 1**) at 10 μM for 2 and 4 hours.

In the MDCKII parental cell line, both Uro-A and Uro-B aglycones showed similar apically and basolaterally directed translocations, with percentages of transport around 20% at 4 h, whereas the transport values for the rest of compounds were lower (**Figure 3A**).

In the murine Bcrp1-transduced MDCKII cell line the most remarkable result was found for Uro-A and Uro-A sulfate in which translocation from the basolateral to the apical compartment significantly increased in comparison with parental cells (**Figure 3B**). The rest of compounds showed no changes in the Bcrp1-transduced MDCKII cell line compared to parental cells. Overall, these results showed an efficient transport of Uro-A by murine Bcrp1 and a moderate transport for its sulfate conjugate in the cell line assayed.

Transport of Uro-A and Uro-A sulfate by human, murine, bovine and ovine BCRP-transduced subclones cells in the absence or presence of Ko143. As the transport of Uro-A by murine Bcrp1-transduced subclone cells was higher than in the rest of compounds, we next determined the vectorial transport of Uro-A (20 μM) across human, murine, bovine and ovine BCRP-transduced MDCKII cells. The transport of Uro-A on all transduced-subclones showed a significant time-dependent increase in the apically directed translocation whereas the basolaterally directed translocation was drastically decreased vs. parental cells (around 10% of transport at 4 h) (**Figure 4**). Among the transduced-subclones, the apically directed translocation of Uro-A was higher on murine Bcrp1 (around 40% of transport at 4 h) followed by ovine BCRP (around 30% of transport at 4 h), human BCRP (around 20% of transport at 4 h) and finally on bovine BCRP (around 16% of transport at 4 h) (**Figure 4**).

In addition, we next confirmed the transport of Uro-A mediated by ABCG2/BCRP performing a co-treatment with a selective BCRP inhibitor, Ko143 (1 μM) on all MDCKII subclones. The BCRP-mediated transport of Uro-A was completely inhibited in all transduced-cells, resulting in a vectorial translocation pattern equal to that of the MDCKII parental cell line (**Figure 4**) and thus confirming that Uro-A is transported by ABCG2/BCRP.

Due to the small available amount of the standard Uro-A sulfate, we focused the study of the transport of this metabolite by only murine Bcrp1 and human BCRP (**Figure 5**). There was a significant increase in the apically directed translocation for Uro-A sulfate using human BCRP-transduced MDCKII cells (2.5-fold increase compared to parental cells; around 50% of transport at 4h), which was higher than that observed for murine Bcrp1 (**Figure 5**). Therefore, these data also confirmed that Uro-A sulfate is also a natural ABCG2/BCRP substrate.

Inhibitory activity evaluation. To show the potential inhibitory effect of urolithins on ABCG2/BCRP, the ability of these compounds to reverse the reduced mitoxantrone (MXR) accumulation in cells transduced with the transporter was tested in flow cytometry experiments. Percentage of inhibition of the different concentrations of Uro-A for Bcrp1/BCRP-transduced cells was related to the effect of reference inhibitor Ko143 (set at 100 % inhibition of ABCG2/BCRP).

Our results showed that Uro-A was able to inhibit ABCG2/BCRP increasing, in a dose-dependent manner, the accumulation of MXR in human BCRP and murine Bcrp1 transduced cells, showing percentages of inhibition of 40-50% at 50 μM (**Figure 6**). This result supported the strong interaction between Uro-A and the transporter showing its important potential as inhibitor since other tested compounds such as urolithins -B, -C and –D, and ellagic acid at 50 and 100 μM did not show any inhibition (data not shown).

DISCUSSION

A number of dietary polyphenols as well as their *in vivo* conjugates, have been reported to be substrates for ABCG2/BCRP transporters, which suggests that this interaction could also modulate the pharmacokinetic behavior and distribution of different drugs.[10,11,13,15,45]

Urolithins are metabolites produced by the gut microbiota from the polyphenols ellagitannins and ellagic acid that could exert biological activity at both systemic and gastrointestinal levels.[46] Uro-A, the most abundant urolithin produced by humans,[46] has been reported to be the most active urolithin with acknowledged *in vitro*[22,23,28,29,32,34] and *in vivo*[31,47] anti-inflammatory and anticarcinogenic activities. Regarding the biological activity of the phase II conjugates, the main

228 *in vivo* circulating conjugate, Uro-A glur, has shown to decrease the TNF-α-induced
229 inflammation in endothelial cells.[35]
230 Taking into account the above, we evaluated whether urolithins and some representative
231 circulating conjugates could be substrates for ABCG2/BCRP at a physiologically relevant
232 concentration (20 μM).[19,22] For this purpose we examined their active transport using a parental
233 and murine Bcrp1-transduced MDCKII cell model. Our results indicated that only Uro-A, and
234 also its sulfate conjugate, showed a significant increase in the apically directed translocation
235 together with a decrease of the basolaterally directed translocation compared to parental cells. In
236 contrast, Bcrp1 showed no affinity for the urolithin precursor EA and the rest of urolithins and
237 glucuronide conjugates.
238 Our results indicate that the affinity of ABCG2/BCRP for urolithins seems to be influenced
239 by the number and position of hydroxyl groups in the urolithin scaffold. In the present study,
240 BCRP only showed affinity for Uro-A, with two hydroxyl groups in 3 and 8-positions (**Figures 1**
241 **and 2**). In this regard, a structure-activity relationships (SAR) study comparing the BCRP
242 inhibitory effect of twelve different flavonoids indicated that flavones were more efficient than
243 flavonols, isoflavones and flavanones due to the occurrence of hydroxyl groups (OH-) at 5-
244 position, in contrast to positions 3 and 7 in flavones.[48] More recently, another SAR study in
245 flavonoids confirmed that OH-group in 5-position contributed positively to BCRP inhibition
246 because the replacement of this OH-group by a 3-methoxy group resulted in a decrease in the
247 affinity.[49] Our results in urolithins also support the potential role of OH-groups in the interaction
248 with BCRP. The presence of an OH-group at 8-position, but not at 3-position, might favor the
249 interaction with BCRP, which was supported by the lack of interaction between BCRP and Uro-
250 B, with only one OH-group at 3-position (**Figure 1**). In the case of urolithin A conjugates (sulfate

and glucuronide), the possible explanation is more difficult. The chemical synthesis of Uro-A glur and Uro-A sulfate yielded a mixture of 50% Uro-A 3-glur and 50% Uro-A 8-glur for the glucuronides and also 50% Uro-A 3-sulfate and 50% Uro-A 8-sulfate in the case of the sulfate conjugate (**Figures 1** and **2**). Therefore, some affinity of BCRP for Uro-A glur should be expected since the 8-position was 50% available, as in the case or Uro-A sulfate. However, whereas Uro-A sulfate was a BCRP substrate, Uro-A glur was not transported at all (**Figure 3**). In addition, the occurrence of additional hydroxyl groups (Uro-C and Uro-D; **Figure 1**) decreased the affinity of BCRP for urolithins. Overall, the above rationale is coincident, at least in part, with that launched in a previous study where estrogenic receptors (alpha and beta) showed higher affinity for Uro-A than for Uro-B.[37] The transport of Uro-A sulfate (**Figure 5**) confirms that ABCG2/BCRP might be a general phytoestrogen transporter for a structurally diverse array of phytoestrogen sulfates including sulfate conjugates of enterolignans, isoflavones, and coumestans, under physiological conditions.[50] Interestingly, it was also found that the inhibitory potency against ABCG2/BCRP of daidzein-7-glucuronide was 100 fold lower than daidzein while daidzein-4-sulfate showed an inhibitory potency comparable to daidzein.[51]

In the present study, the affinity of ABCG2/BCRP for Uro-A was also confirmed for bovine and ovine BCRP as well as for human BCRP transporters in the line of recent studies that have included the comparative inhibition among murine Bcrp1, bovine and ovine BCRP, and human BCRP.[13,41,52,53] *In vitro* results showed an efficient and dose-dependent inhibition of Uro-A with percentages observed of 40-50% with a concentration of 50 μM for human BCRP and murine Bcrp1 in mitoxantrone accumulation assays, in agreement with known BCRP inhibitors such as the flavonoid biochanin A.[54] In addition, these data showed the potential of Uro-A as a reversal agent in chemotherapy treatments with regard to the multidrug resistance (MDR) phenotype.[7]

These results indicate that urolithins, also produced by cattle,[24,55] could interact with BCRP affecting oral bioavailability of drugs (antibiotics and others) and drug transport across barriers as previously described in cattle for the isoflavones genistein and daidzein.[9] On the other hand, the contribution of the phytochemical-glucuronide transport by ABCC2/MRP2 and ABCC3/MRP3[14,56] should be considered in further studies taken into account the plasma metabolic profile of urolithins.[16]

The present study shows, for the first time, that Uro-A and Uro-A-sulfate are transported by ABCG2/BCRP in the apically directed translocation. Moreover, Uro-A acts as inhibitor of the transporter *in vitro*. On the contrary, the urolithin precursor EA as well as the urolithins Uro-B, -C, -D, and the phase II conjugates Uro-A glur and Uro-B glur were not transported. It has been reported that the dietary consumption of ellagitannin- or ellagic acid-containing foods (pomegranate, strawberries, walnuts, etc.) can exert anti-inflammatory effects due to the *in vivo* formation of Uro-A by the gut microbiota.[31,46] However, the results obtained here also suggest that Uro-A might influence the pharmacokinetics and bioavailability of drug levels which could lead to potential adverse effects. Therefore, further *in vivo* studies should clarify this hypothesis.

ABBREVIATIONS USED

ABC, ATP-binding cassette; CAN, acetonitrile; BCRP, breast cancer resistance protein; cDNA, complementary deoxyribonucleic acid; DIPEA, N,N-diisopropylethylamine; DMSO, dimethyl sulfoxide; EA, ellagic acid; Glur, glucuronide; HPLC, High-performance liquid chromatography; MDCKII, Mardin-Darby canine kidney; MDR, multidrug resistance; MeOH, methanol; MRP, multidrug resistant protein; MXR, mitoxantrone; OH-, hydroxyl group; SD, standard deviation; SIM, selective ion monitoring; SAR; structure-activity relationship; TBDMS, *tert*-butyldimethylsilyl; TNF-α, Tumor necrosis factors-alpha; Uro-, urolithin.

FUNDING INFORMATION

This work was funded by the Projects CICYT ALG2011-22447, AGL2012-31116, Consolider Ingenio 2010, CSD2007-00063 (Fun-*C*-Food), and Fundación Seneca de la Región de Murcia, Spain (Grupo de Excelencia GERM 06 04486 and 05556/PI/04).

CONFLICT OF INTEREST

The authors declare no competing financial interest.

SUPPORTING INFORMATION AVAILABLE

This material is available free of charge via the Internet at http://pubs.acs.org.

Supplementary Methods. Experimental procedure for the synthesis of Uro-A glucuronide and Uro-A sulfate.

REFERENCES

(1) Borst, P.; Elferink, R. O. Mammalian ABC transporters in health and disease. *Annu. Rev. Biochem*. **2002**, *71*, 537–592.

(2) Glavinas, H.; Krajcsi, P.; Cserepes, J.; Sarkadi, B. The role of ABC transporters in drug resistance, metabolism and toxicity. *Curr. Drug Deliv*. **2004**, *1*, 27–42.

(3) Krishnamurthy, P.; Schuetz, J. D. Role of ABCG2/BCRP in biology and medicine. *Annu. Rev. Pharmacol. Toxicol*. **2006**, *46*, 381–410.

(4) Glavinas, H.; Kis, E.; Pál, A.; Kovács, R.; Jani, M.; Vági, E.; Molnár, E.; Bánsághi, S.; Kele, Z.; Janáky, T.; Báthori, G.; von Richter, O.; Koomen, G. J.; Krajcsi, P. ABCG2 (breast cancer resistance protein/mitoxantrone resistance-associated protein) ATPase assay: a useful tool to detect drug-transporter interactions. *Drug Metab. Dispos*. **2007**, *35*, 1533–1542.

(5) Huang, Y.; Sadée, W. Membrane transporters and channels in chemoresistance and -sensitivity of tumor cells. *Cancer Letters* **2006**, *239*, 168–182.

(6) de Wolf, C.; Jansen, R.; Yamaguchi, H.; de Haas, M.; van de Wetering, K.; Wijnholds, J.; Beijnen, J.; Borst, P. Contribution of the drug transporter ABCG2 (breast cancer resistance protein) to resistance against anticancer nucleosides. *Mol. Cancer Ther*. **2008**, *7*, 3092–3102.

(7) Fukuda, Y.; Schuetz, J. D. ABC transporters and their role in nucleoside and nucleotide drug resistance. *Biochem. Pharmacol*. **2012**, *83*, 1073-1083.

(8) van de Wetering, K.; Burkon, A.; Feddema, W.; Bot, A.; de Jonge, H.; Somoza, V.; Borst, P. Intestinal breast cancer resistance protein (BCRP)/Bcrp1 and multidrug resistance protein 3 (MRP3)/Mrp3 are involved in the pharmacokinetics of resveratrol. *Mol. Pharmacol*. **2009,** *75*, 876-885.

(9) Merino, G.; Pérez, M.; Real, R.; Egido, E.; Prieto, J. G.; Álvarez, A. I. *In vivo* inhibition of BCRP/ABCG2 mediated transport of nitrofurantoin by the isoflavones genistein and daidzein: A comparative study in Bcrp1(−/−) mice. *Pharm. Res*. **2010**, *27*, 2098–2105

(10) Álvarez, A. I.; Real, R.; Pérez, M.; Mendoza, G.; Prieto, J. G.; Merino, G. Modulation of the activity of ABC transporters (P-glycoprotein, MRP2, BCRP) by flavonoids and drug response. *J. Pharm. Sci*. **2010**, *99*, 598-617.

(11) Li, Y.; Lu, J.; Paxton, J. W. The role of ABC and SLC transporters in the pharmacokinetics of dietary and herbal phytochemicals and their interactions with xenobiotics. *Curr. Drug Metab*. **2012**, *13*, 624-639.

(12) Álvarez, A.I.; Vallejo, F.; Barrera, B.; Merino, G.; Prieto, J. G.; Tomás-Barberán, F. A.; Espín, J. C. Bioavailability of the glucuronide and sulfate conjugates of genistein and daidzein in breast cancer resistance protein 1 knockout mice. *Drug Metab. Dispos.* **2011**, *39*, 2008-2012.

(13) Pérez, M.; Otero, J. A.; Barrera, B.; Prieto, J.G.; Merino, G.; Álvarez, A. I. Inhibition of ABCG2/BCRP transporter by soy isoflavones genistein and daidzein: Effect on plasma and milk levels of danofloxacin in sheep. *Vet. J*. **2012**, pii: S1090-0233(12)00397-8.

(14) Weing, J.; Hu, M. Mutual interactions between flavonoids and enzymatic and transporter elements responsible for flavonoid disposition via phase II metabolic pathways. *RSC Advances* **2012**, *2*, 7948-7963.

(15) Alfaras. I.; Pérez, M.; Juan, M. E.; Merino, G.; Prieto, J. G.; Planas, J. M.; Álvarez, A. I. Involvement of breast cancer resistance protein (BCRP1/ABCG2) in the bioavailability and tissue distribution of trans-resveratrol in knockout mice. *J. Agric. Food Chem*. **2010**, *58*, 4523-4528.

(16) Cerdá, B.; Espín, J. C.; Parra, S.; Martínez, P.; Tomás-Barberán, F. A. The potent *in vitro* antioxidant ellagitannins from pomegranate juice are metabolised into bioavailable but poor

359 antioxidant hydroxy-6H-dibenzopyran-6-one derivatives by the colonic microflora of healthy
360 humans. *Eur. J. Nutr*. **2004**, *43*, 205-220.
361 (17) Cerdá, B.; Periago, P. M.; Espín, J. C.; Tomás-Barberán, F. A. Identification of urolithin
362 A as a metabolite produced by human colon microflora from ellagic acid and related compounds
363 *J. Agric. Food Chem*. **2005**, *53*, 5571– 5576
364 (18) Cerdá, B.; Tomás-Barberán, F. A.; Espín, J. C. Metabolism of antioxidant and
365 chemopreventive ellagitannins from strawberries, raspberries, walnuts, and oak-aged wine in
366 humans: identification of biomarkers and individual variability. *J. Agric. Food Chem*. 2005; *53*,
367 227-235.
368 (19) Espín, J. C.; González-Barrio, R.; Cerdá, B.; López-Bote, C.; Rey, A. I.; Tomás-Barberán,
369 F. A. Iberian pig as a model to clarify obscure points in the bioavailability and metabolism of
370 ellagitannins in humans *J. Agric. Food Chem*. **2007**, *55*, 10476– 10485.
371 (20) Cerdá, B.; Llorach, R.; Cerón, J. J.; Espín, J. C.; Tomás-Barberán, F. A. Evaluation of the
372 bioavailability and metabolism in the rat of punicalagin, an antioxidant polyphenol from
373 pomegranate juice. *Eur. J. Nutr*. **2003**, *42*, 18-28.
374 (21) Ito, H.; Iguchi, A.; Hatano, T. Identification of urinary and intestinal bacterial metabolites
375 of ellagitannin geraniin in rats. *J. Agric. Food Chem*. **2008**, *56*, 393–400.
376 (22) González-Sarrías, A.; Azorín-Ortuño, M.; Yáñez-Gascón, M. J.; Tomás-Barberán, F. A.;
377 García-Conesa, M. T.; Espín, J. C. Dissimilar *in vitro* and *in vivo* effects of ellagic acid and its
378 microbiota-derived metabolites, urolithins, on the cytochrome P450 1A1. *J. Agric. Food Chem*.
379 **2009**, *57*, 5623-5632.
380 (23) Seeram, N. P.; Aronson, W. J.; Zhang, Y.; Henning, S. M.; Moro, A.; Lee, R. P.;
381 Sartippour, M.; Harris, D. M.; Rettig, M.; Suchard, M. A.; Pantuck, A. J.; Belldegrun, A.; Heber,

382 D. Pomegranate ellagitannin-derived metabolites inhibit prostate cancer growth and localize to
383 the mouse prostate gland. *J. Agric. Food Chem*. **2007**, *55*, 7732-7737.
384 (24) González-Barrio, R.; Truchado, P.; Ito, H.; Espín, J. C.; Tomás-Barberán, F. A. UV and
385 MS identification of urolithins and nasutins, the bioavailable metabolites of ellagitannins and
386 ellagic acid in different mammals *J. Agric. Food Chem*. **2011**, *59*, 1152– 1162.
387 (25) Cerdá, B.; Soto, C.; Albaladejo, M. D.; Martínez, P.; Sánchez-Gascón, F.; Tomás-
388 Barberán, F.; Espín, J. C. Pomegranate juice supplementation in chronic obstructive pulmonary
389 disease: a 5-week randomized, double-blind, placebo-controlled trial. *Eur. J. Clin. Nutr*. **2006**,
390 *60*, 245-253.
391 (26) Truchado, P.; Larrosa, M.; García-Conesa, M. T.; Cerdá, B.; Vidal-Guevara, M. L.;
392 Tomás-Barberán, F. A.; Espín, J. C. Strawberry processing does not affect the production and
393 urinary excretion of urolithins, ellagic acid metabolites, in humans. *J. Agric. Food Chem*. **2011**,
394 *60*, 5749-5754.
395 (27) González-Sarrías, A.; Giménez-Bastida, J. A.; García-Conesa, M. T.; Gómez-Sánchez, M.
396 B.; García-Talavera, N. V.; Gil-Izquierdo, A.; Sánchez-Alvarez, C.; Fontana-Compiano, L. O.;
397 Morga-Egea, J. P.; Pastor-Quirante, F. A.; Martínez-Díaz, F.; Tomás-Barberán, F. A.; Espín, J.C.
398 Occurrence of urolithins, gut microbiota ellagic acid metabolites and proliferation markers
399 expression response in the human prostate gland upon consumption of walnuts and pomegranate
400 juice. *Mol. Nutr. Food Res*. **2010**, *54*, 311– 322
401 (28) González-Sarrías, A.; Espín, J. C.; Tomás-Barberán, F. A.; García-Conesa, M. T. Gene
402 expression, cell cycle arrest and MAPK signalling regulation in Caco-2 cells exposed to ellagic
403 acid and its metabolites, urolithins. *Mol. Nutr. Food Res*. **2009**, *53*, 686-698.

(29) Sharma, M.; Li, L.; Celver, J.; Killian, C.; Kovoor, A.; Seeram, N. P. Effects of fruit ellagitannin extracts, ellagic acid, and their colonic metabolite, urolithin A, on Wnt signaling. *J. Agric. Food Chem*. **2010**, *58*, 3965-3969.

(30) Kasimsetty, S. G.; Bialonska, D.; Reddy, M. K.; Ma, G.; Khan, S. I.; Ferreira, D. Colon cancer chemopreventive activities of pomegranate ellagitannins and urolithins. *J. Agric. Food Chem*. **2010**, *58*, 2180-2187.

(31) Larrosa, M.; González-Sarrías, A.; Yáñez-Gascón, M.J.; Selma, M. V.; Azorín-Ortuño, M.; Toti, S.; Tomás-Barberán, F.; Dolara, P.; Espín, J. C. Anti-inflammatory properties of a pomegranate extract and its metabolite urolithin-A in a colitis rat model and the effect of colon inflammation on phenolic metabolism. *J. Nutr. Biochem*. **2010**; *21*, 717-725.

(32) González-Sarrías, A.; Larrosa, M.; Tomás-Barberán, F. A.; Dolara, P.; Espín, J. C. NF-kappaB-dependent anti-inflammatory activity of urolithins, gut microbiota ellagic acid-derived metabolites, in human colonic fibroblasts. *Br. J. Nutr*. **2010**; *104*, 503-512.

(33) Verzelloni, E.; Pellacani, C.; Tagliazucchi, D.; Tagliaferri, S.; Calani, L.; Costa, L. G.; Brighenti, F.; Borges, G.; Crozier, A.; Conte, A.; Del Rio, D. Antiglycative and neuroprotective activity of colon-derived polyphenol catabolites. *Mol. Nutr. Food Res*. **2011**, *55*, S35-S43.

(34) Giménez-Bastida, J. A.; Larrosa, M.; González-Sarrías, A.; Tomás-Barberán, F.; Espín, J. C.; García-Conesa, M. T. Intestinal Ellagitannin Metabolites Ameliorate Cytokine-Induced Inflammation and Associated Molecular Markers in Human Colon Fibroblasts. *J. Agric. Food Chem*. **2012**, *60*, 8866-8876.

(35) Giménez-Bastida, J. A.; González-Sarrías, A.; Larrosa, M.; Tomás-Barberán, F.; Espín, J. C.; García-Conesa, M. T. Ellagitannin metabolites, urolithin A glucuronide and its aglycone urolithin A, ameliorate TNF-α-induced inflammation and associated molecular markers in human aortic endothelial cells. *Mol. Nutr. Food Res*. **2012**, *56*, 784-796.

(36) Giménez-Bastida, J. A.; Truchado, P.; Larrosa, M.; Espín, J. C.; Tomás-Barberán, F. A.; Allende, A.; García-Conesa, M. T. Urolithins, ellagitannin metabolites produced by colon microbiota, inhibit Quorum Sensing in Yersinia enterocolitica: Phenotypic response and associated molecular changes. *Food Chem*. **2012**, *132*, 1465-1474.

(37) Larrosa, M.; González-Sarrías, A.; García-Conesa, M. T.; Tomás-Barberán, F. A.; Espín, J. C. Urolithins, ellagic acid-derived metabolites produced by human colonic microflora, exhibit estrogenic and antiestrogenic activities. *J. Agric. Food Chem*. **2006**, *54*, 1611-1620.

(38) Bialonska, D.; Kasimsetty, S. G.; Khan, S. I.; Ferreira, D. Urolithins, intestinal microbial metabolites of Pomegranate ellagitannins, exhibit potent antioxidant activity in a cell-based assay. *J. Agric. Food Chem*. **2009**, *57*, 10181-10186.

(39) Lucas, R.; Alcantara, D.; Morales, J. C. A concise synthesis of glucuronide metabolites of urolithin-B, resveratrol, and hydroxytyrosol. *Carbohydr. Res*. **2009**, *344*, 1340-1346.

(40) Tanis, V. M.; Moya, C.; Jacob, R. S.; Little, R. D. Synthesis and evaluation of the bioactivity of simplified analogs of the seco-pseudopterosins; progress toward determining a pharmacophore. *Tetrahedron* **2008**, *64*, 10649-10663.

(41) Real, R.; González-Lobato, L.; Baro, M. F.; Valbuena, S.; de la Fuente, A.; Prieto, J. G.; Álvarez, A. I.; Marqués, M. M.; Merino, G. Analysis of the effect of the bovine ABCG2 SNP Y581S on transcellular transport of veterinary drugs using new cell culture models. *J. Anim. Sci*. **2011**, *89*, 4325–4338.

(42) González-Lobato, L.; Real, R.; Herrero, D.; de la Fuente, A.; Prieto, J. G.; Márques, M. M.; Álvarez, A. I.; Merino, G. Identification of substrates and inhibitors of the ovine and bovine adenosine triphosphate-binding cassette transporter G2: interaction with veterinary drugs, micronutrients and natural products. *Submitted to Journal of Animal Science*.

(43) Jonker, J. W.; Smit, J. W.; Brinkhuis, R. F.; Maliepaard, M.; Beijnen, J. H.; Schellens, J. H.; Schinkel, A. H. Role of breast cancer resistance protein in the bioavailability and fetal penetration of topotecan. *J. Natl. Cancer Inst*. **2000**, *92*, 1651–1656.

(44) Pavek, P.; Merino, G.; Wagenaar, E.; Bolscher, E.; Novotna, M.; Jonker, J. W.; Schinkel, A. H. Human breast cancer resistance protein: interactions with steroid drugs, hormones, the dietary carcinogen 2-amino-1-methyl-6-phenylimidazo(4,5-b)pyridine, and transport of cimetidine. *J. Pharmacol. Exp. Ther*. **2005**, *312*, 144-152.

(45) Zhang, S.; Yang, X.; Morris, M. E. Combined effects of multiple flavonoids on breast cancer resistance protein (ABCG2)-mediated transport. *Pharm. Res*. **2004**, *21*, 1263–1273.

(46) Larrosa, M.; García-Conesa, M.T.; Espín, J.C.; Tomás-Barberán, F.A. Ellagitannins, ellagic acid and vascular health. *Mol. Asp. Med.* **2010**, *31*, 513-39.

(47) Ishimoto, H.; Shibata, M.; Myojin, Y.; Ito, H.; Sugimoto, Y.; Tai, A.; Hatano, T. *In vivo* anti-inflammatory and antioxidant properties of ellagitannin metabolite urolithin A. *Bioorg. Med. Chem. Lett.* **2011**, *21*, 5901-5904.

(48) Ahmed-Belkacem, A.; Pozza, A.; Munoz-Martinez, F.; Bates, S. E.; Castanys, S.; Gamarro, F.; Di Pietro, A.; Perez-Victoria, J. M. Flavonoid structure-activity studies identify 6-prenylchrysin and tectochrysin as potent and specific inhibitors of breast cancer resistance protein ABCG2. *Cancer Res*. **2005**, *65*, 4852–4860.

(49) Pick, A.; Müller, H.; Mayer, R.; Haenisch, B.; Pajeva, I. K.; Weigt, M.; Bönisch, H.; Müller, C. E.; Wiese, M. Structure-activity relationships of flavonoids as inhibitors of breast cancer resistance protein (BCRP). *Bioorg. Med. Chem*. **2011**, *19*, 2090-2102.

(50) van de Wetering, K.; Sapthu, S. ABCG2 functions as a general phytoestrogen sulfate transporter *in vivo*. *FASEB J*. **2012**, *26*, 4014-4024.

(51) Tamaki, H.; Satoh, H.; Hori, S.; Ohtani, H.; Sawada, Y. Inhibitory effects of herbal extracts on breast cancer resistance protein (BCRP) and structure-inhibitory potency relationship of isoflavonoids. *Drug Metab. Pharmacokinet*. **2010**, *25*, 170-179.

(52) González-Lobato, L.; Real, R.; Prieto, J. G.; Álvarez, A. I.; Merino, G. Differential inhibition of murine Bcrp1/Abcg2 and human BCRP/ABCG2 by the mycotoxin fumitremorgin C. *Eur. J. Pharmacol*. **2010**, *644*, 41-48.

(53) Otero, J. A.; Real, R.; de la Fuente, A.; Prieto, J. G.; Marques, M.; Álvarez, A. I.; Merino, G. The bovine ATP-binding cassette transporter ABCG2 Y581S single nucleotide polymorphism increases milk secretion of the fluoroquinolone danofloxacin. *Drug Metab. Dispos*. **2012**, doi:10.1124/dmd.112.049056.

(54) Ang, G.; Morris, M. E. Effects of the isoflavonoid biochanin A on the transport of mitoxantrone *in vitro* and *in vivo*. *Biopharm. Drug Dispos*. **2010**, *31*, 340-350.

(55) González-Barrio, R.; Truchado, P.; García-Villalba, R.; Hervás, G.; Frutos, P.; Espín, J. C.; Tomás-Barberán, F. A. Metabolism of oak leaf ellagitannins and urolithin production in beef cattle. *J. Agric. Food Chem*. **2012**, *60*, 3068-3077.

(56) van de Wetering, K.; Feddema, W.; Helms, J. B.; Brouwers, J. F.; Borst, P. Targeted metabolomics identifies glucuronides of dietary phytoestrogens as a major class of MRP3 substrates *in vivo*. *Gastroenterology* **2009**, *137*, 1725-1735.

FIGURE CAPTIONS

Figure 1. Chemical structures of EA, Uro-D, Uro-C, Uro-A, Uro-B. The arrows designate the sequence of metabolic steps carried out by the gut microbiota.

Figure 2. (**A**) Synthesis of Uro-A glucuronates; a) TBDMSTfO, DIPEA (N,N-diisopropylethylamine), CH_2Cl_2; b) BF_3•OEt_2; CH_2Cl_2, glucuronate donor **3**; c) K_2CO_3, KF, MeOH-H_2O (5:1). (**B**) Synthesis of Uro-A sulfates; d) SO_3•NMe_3, NEt_3, CH_3CN, 100 ºC, 20 min, MW; e) KF, MeOH.

Figure 3. Transepithelial transport of tested compounds (10 μM) in (A) parental MDCKII cells and in (B) their murine Bcrp1-transduced derivatives. The experiment was started with the addition of each compound to one compartment (basolateral or apical). After 2 and 4 h, the percentage of each compound appearing in the opposite compartment was measured by LC-MS and plotted. Data are expressed as mean values ± SD (n = 3). (○) Translocation from the basolateral to the apical compartment; (●) translocation from the apical to the basolateral compartment.

Figure 4. Transepithelial transport of Uro-A (20 μM) in parental MDCKII cells, and in their murine Bcrp1-, and human, bovine and ovine BCRP-transduced subclones in the absence or presence of Ko143 (1 μM). The experiment was carried out as indicated in **Figure 2**. Data are expressed as mean values ± SD (n = 3). ○, Translocation from the basolateral to the apical compartment; ●, translocation from the apical to the basolateral compartment.

518 **Figure 5.** Transepithelial transport of Uro-A sulfate (20 μM) in parental MDCKII, and in their
519 murine Bcrp1- and human BCRP-transduced derivatives. The experiment was carried out as
520 indicated in Figure 2. Data are expressed as mean values ± SD (n = 3). ○, Translocation from the
521 basolateral to the apical compartment; ●, translocation from the apical to the basolateral
522 compartment.
523
524 **Figure 6.** Percentage of inhibition of the different concentrations of Uro-A for Bcrp1/BCRP-
525 transduced cells in mitoxantrone accumulation assays. Data are expressed as mean values ± SD
526 (n = 3). Percentage of inhibition was related to the effect of reference inhibitor Ko143 (set at 100
527 % inhibition of ABCG2/BCRP).

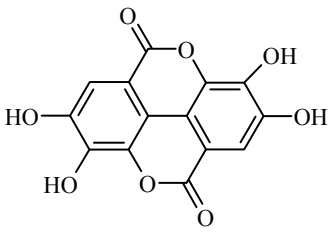

Ellagic acid (EA); M-H=301

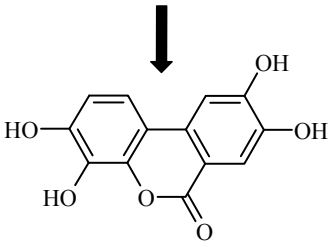

Urolithin D (Uro-D); M-H=259

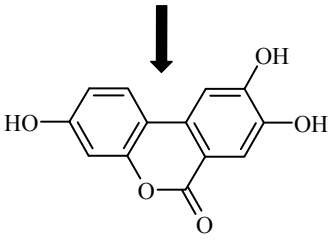

Urolithin C (Uro-C); M-H=243

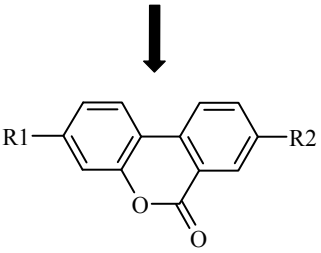

R1 = OH and R2 = OH; Urolithin A (Uro-A); M-H=227
R1 or R2 = OH, and R1 or R2 = Glucuronic acid; Urolithin A glucuronide (Uro-A glur); M-H=403
R1 or R2 = OH, and R1 or R2 = Sulfate; Urolithin A sulfate (Uro-A sulfate); M-H=307

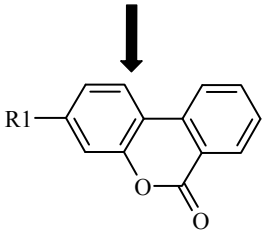

R1 = OH; Urolithin B (Uro-B); M-H=211
R1 = Glucuronic acid; Urolithin B glucuronide (Uro-B glur); M-H=387

Figure 1.

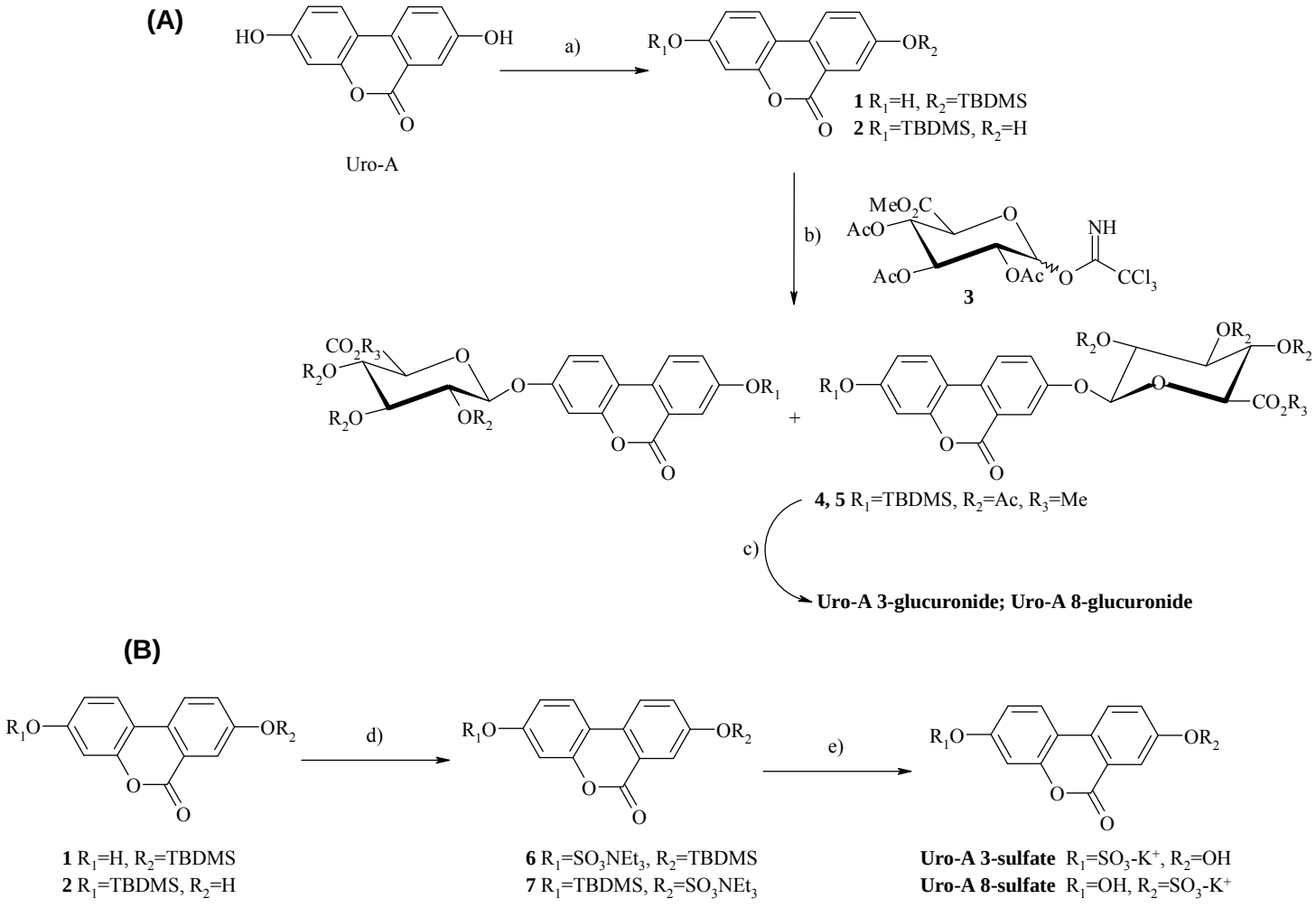
(A)
HO
OH
Uro-A
a)
R1O
OR2
1 R1=H, R2=TBDMS
2 R1=TBDMS, R2=H
b)
MeO2C
AcO
AcO
OAc
NH
CCl3
3
CO2R3
R2O
R2O
OR2
OR1
+
OR2
CO2R3
4, 5 R1=TBDMS, R2=Ac, R3=Me
c)
Uro-A 3-glucuronide; Uro-A 8-glucuronide
(B)
d)
e)
1 R1=H, R2=TBDMS
2 R1=TBDMS, R2=H
6 R1=SO3NEt3, R2=TBDMS
7 R1=TBDMS, R2=SO3NEt3
Uro-A 3-sulfate R1=SO3-K+, R2=OH
Uro-A 8-sulfate R1=OH, R2=SO3-K+

Figure 2

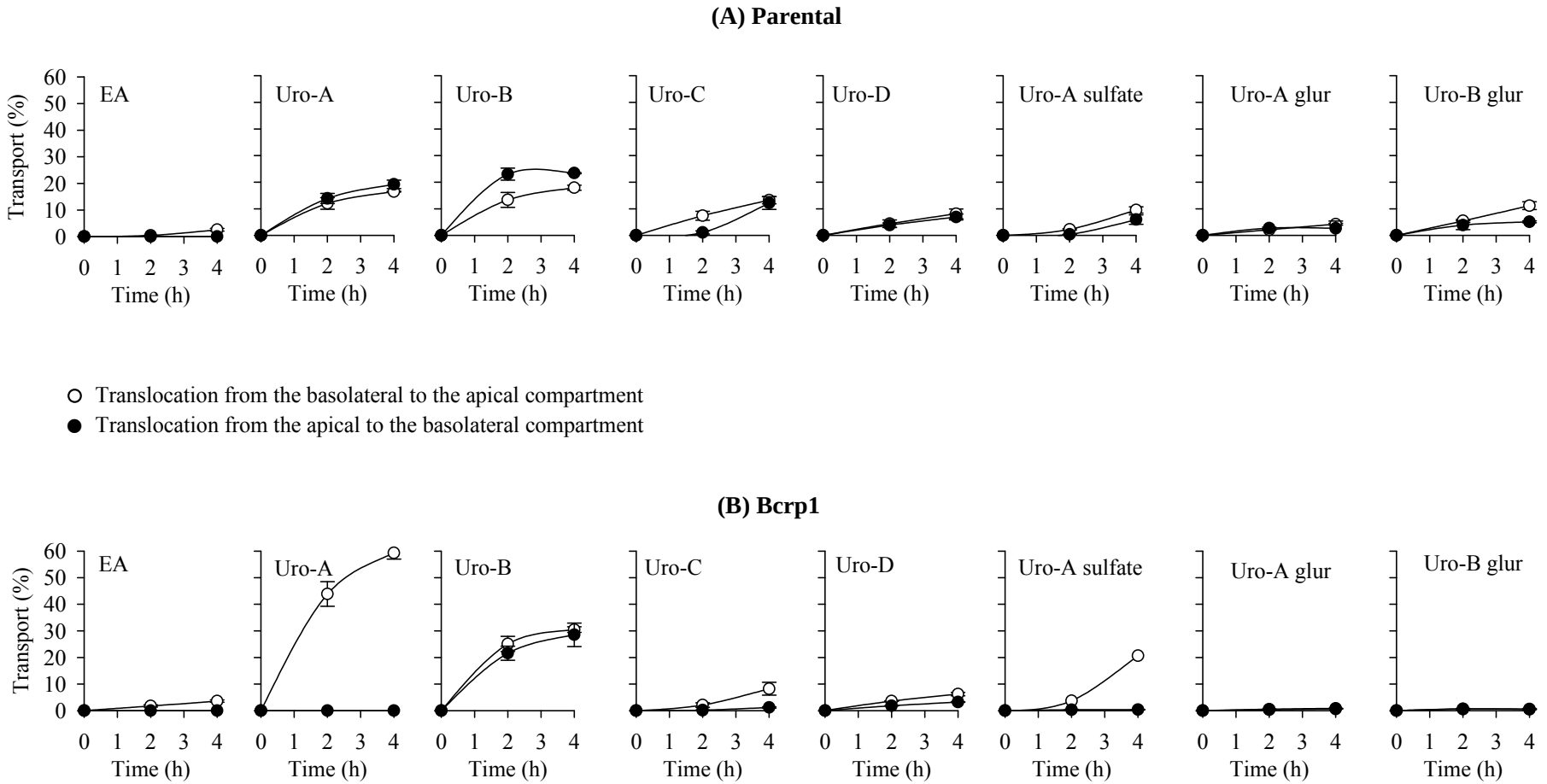
(A) Parental
EA
Uro-A
Uro-B
Uro-C
Uro-D
Uro-A sulfate
Uro-A glur
Uro-B glur
Transport (%)
Time (h)
Translocation from the basolateral to the apical compartment
Translocation from the apical to the basolateral compartment
(B) Bcrp1
EA
Uro-A
Uro-B
Uro-C
Uro-D
Uro-A sulfate
Uro-A glur
Uro-B glur
Transport (%)
Time (h)

Figure 3.

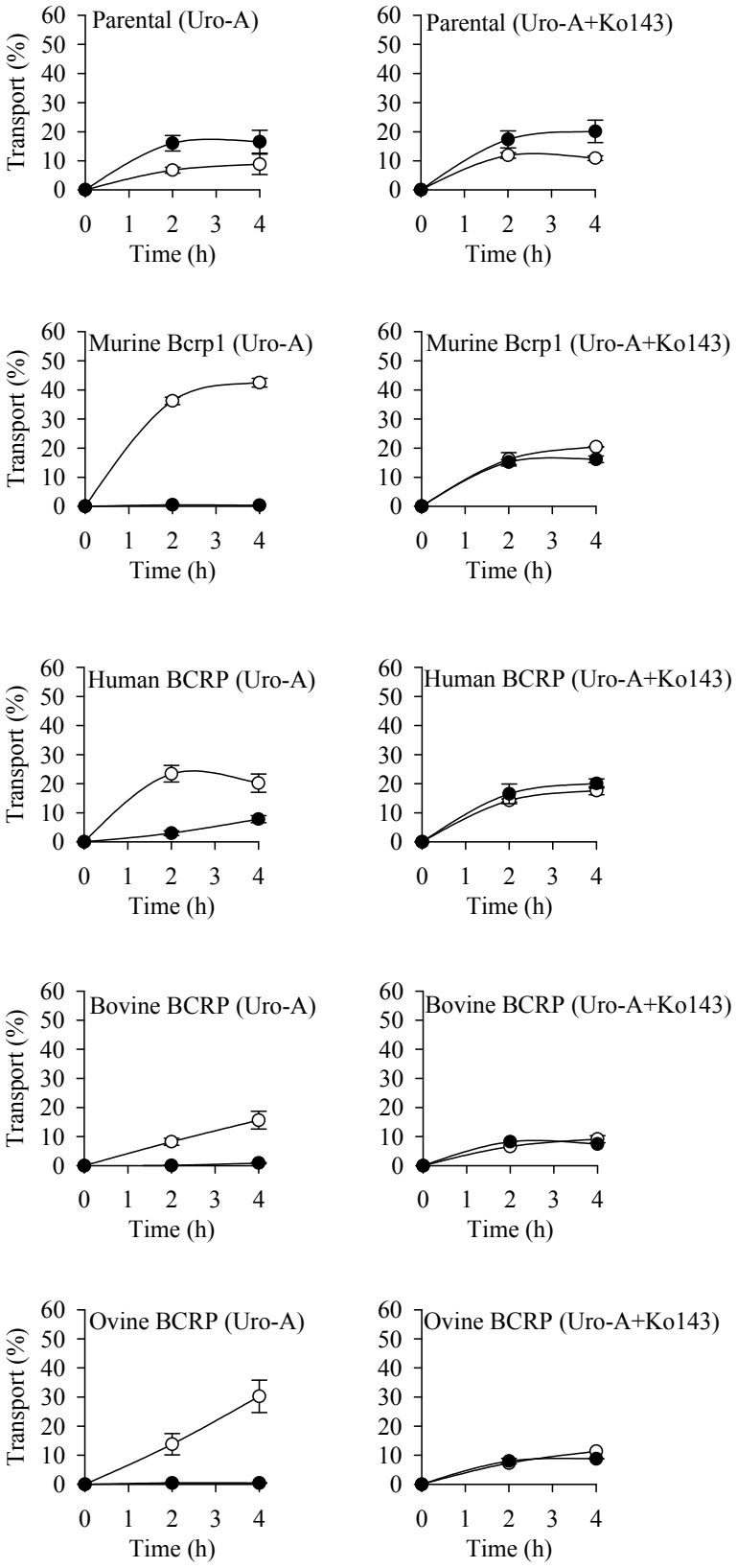
Parental (Uro-A)
Parental (Uro-A+Ko143)
Murine Bcrp1 (Uro-A)
Murine Bcrp1 (Uro-A+Ko143)
Human BCRP (Uro-A)
Human BCRP (Uro-A+Ko143)
Bovine BCRP (Uro-A)
Bovine BCRP (Uro-A+Ko143)
Ovine BCRP (Uro-A)
Ovine BCRP (Uro-A+Ko143)
Transport (%)
Time (h)
0 10 20 30 40 50 60
0 1 2 3 4

Figure 4.

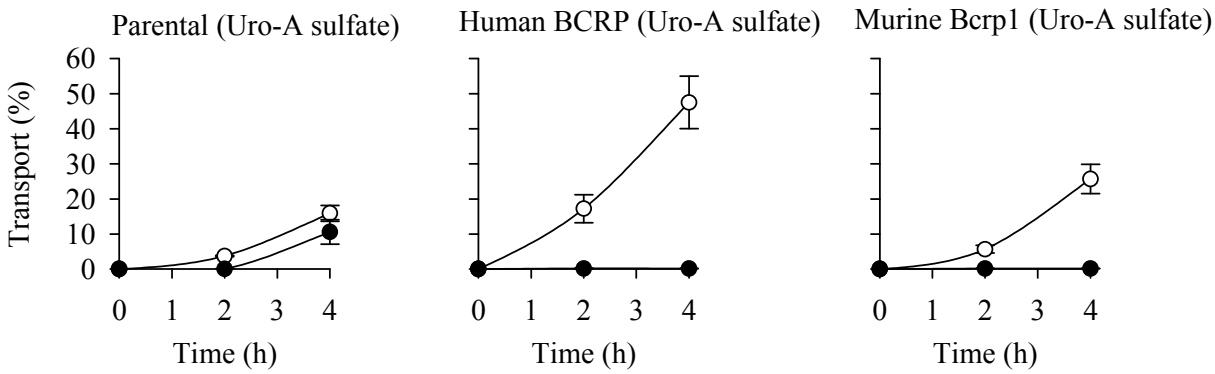
Parental (Uro-A sulfate)
Human BCRP (Uro-A sulfate)
Murine Bcrp1 (Uro-A sulfate)
Transport (%)
60
50
40
30
20
10
0
0 1 2 3 4
Time (h)

Figure 5

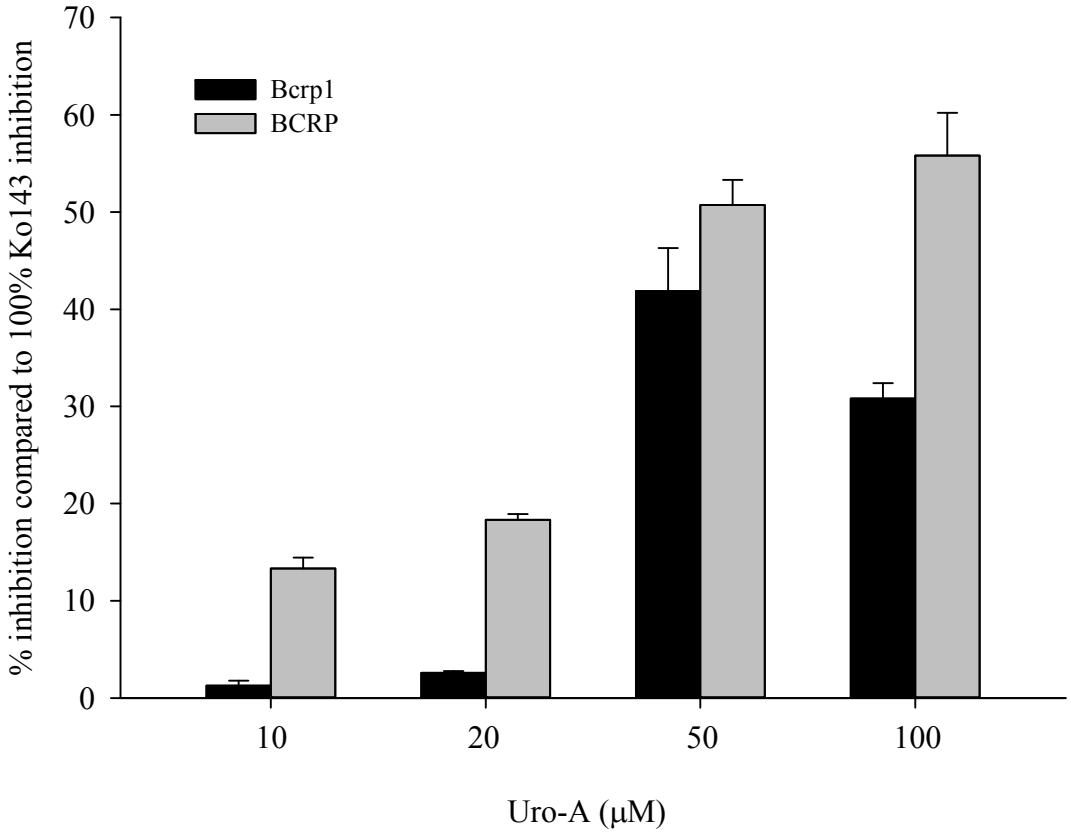
70
60
50
40
30
20
10
0
% inhibition compared to 100% Ko143 inhibition
Bcrp1
BCRP
10
20
50
100
Uro-A (μM)

Figure 6.

Graphical Abstract

The gut microbiota ellagic acid-derived metabolite urolithin A, and its sulfate conjugate, are substrates for the drug efflux transporter breast cancer resistance protein (ABCG2/BCRP).